Approaches Toward Efficient and Stable Electron Extraction Contact in Organic Photovoltaic Cells: Inspiration from Organic Light-Emitting Diodes

Tae-Woo Lee,* **Kyung-Guen Lim, and Dong-Hun Kim**

Department of Materials Science and Engineering, Pohang University of Science and Technology,
San 31 Hyoja-dong, Nam-gu, Pohang-si, Gyungbuk 790-784, Korea

Electron extraction contact in organic photovoltaic cells (OPVs) is very important to extract electrons from the active layer efficiently, improve the open-circuit voltage, and thus improve the power conversion efficiency. This paper reviews the various approaches to form an electron extraction contact for better power conversion efficiency and device lifetime, especially in organic bulk heterojunction photovoltaic cells based on conjugated polymer: fullerene blends. We discuss the roles of thin metal fluorides, a thin polymeric layer, and a solution processed metal oxide layer at the interface between the photoactive layer and the negative electrode for efficient and stable electron extraction contact in OPVs. In addition, we discuss the effects of various metallic negative electrodes in OPVs in terms of device efficiency and stability. Since these approaches are well established in organic light-emitting diodes, they can be exploited to accelerate research in device engineering to improve device performance.

Keywords: organic solar cells, bulk heterojunction solar cells, electron extraction layer, negative electrode, power conversion efficiency

1. INTRODUCTION

Charge injection or extraction in organic devices such as organic light-emitting diodes (OLEDs) and organic photovoltaic cells (OPVs) has been an important issue, because the device efficiency is critically dependant on the charge injection or extraction contacts.[1-12] Most device design approaches for efficient electron extraction in OPVs have strong similarities to those for efficient electron injection in OLEDs. As many different approaches have been reported to improve the electron injection and the device luminous efficiency in OLEDs, the device engineering in OLEDs can be extended to design high performance OPVs. State-of-art small-molecule OLED devices currently employ metal fluorides,[6] *n*-type layers (*n*-doped electron transport layer),[13] and mixed electron transport layers[14] prior to deposition of the Al cathode to complete the devices. State-of-art polymer light-emitting diodes mostly use low work function metals and metal fluorides/Al as the cathode without an additional electron injection layer to achieve maximum luminous efficiency and device lifetime.[6]

In OPVs, the device design concept for efficient charge extraction (hole and electron extraction) has not yet been well established as most research has focused on the active layer materials and morphologies, as shown in Fig. 1. Among studies in the past five years related to organic photovoltaic cells, papers addressing charge extraction layers and electrodes accounted for 5% and 2%, respectively, as determined from statistics on the ISI web of knowledge database (Thomson Reuters).[15] This can be attributed to the fact that, at this growing stage of research in OPVs, improvement of the overall device power conversion efficiency (PCE) has been improved more rather by optimizing the active material and *p-n* junction morphology than through advances related to the charge extraction layers and electrodes. In particular, recent progress during the past two years on active materials
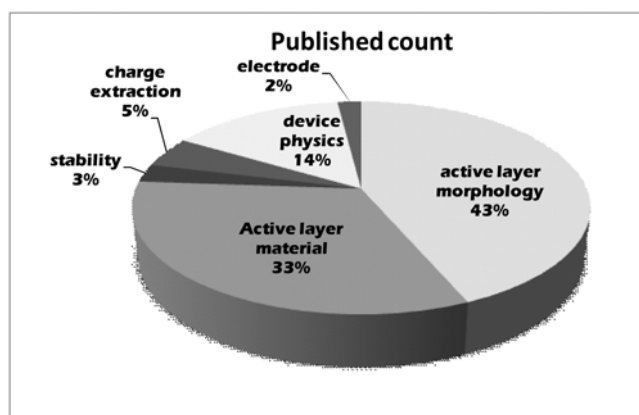

Fig. 1. The statistics of published papers for recent 5 years related to organic photovoltaic cells ('2004-'2008).
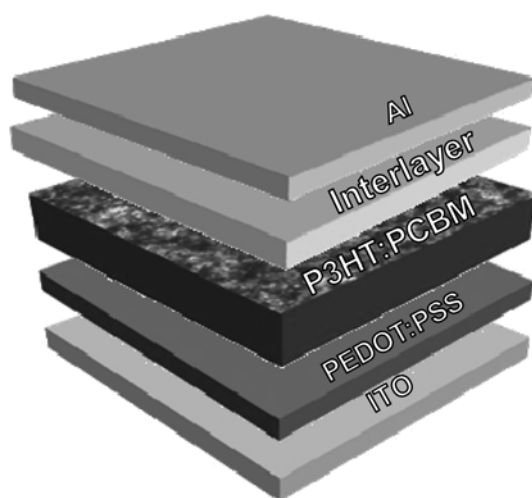
*Corresponding author: twlee@postech.ac.kr

Fig. 2. The basic device structure of organic bulk heterojunction photovoltaic cells based on P3HT: PCBM.

in organic bulk heterojunction solar cells based on polymeric donor materials has been extremely rapid. It is thus anticipated that device engineering to optimize the charge extraction contacts in OPVs with an optimized active layer will becoming increasingly important to further increase the power conversion efficiencies in OPVs.

Figure 2 shows the basic structure of organic solar cells based on a solution process by using a poly(3-hexylthiophene)(P3HT): [6,6]-phenyl-C61-butyric acid methyl ester (PCBM) blend as an active layer and Poly(3,4-ethylenedioxythiophene):poly(styrenesulfonate) (PEDOT:PSS) as the hole extraction buffer layer. The electron extraction and built-in potential can be controlled by using an interfacial layer (or interlayer) in the devices. The various approaches to extract the electrons from the active layer efficiently and increase the open-circuit voltages in OPVs can be categorized into two major groups: (i) use of a non-metallic interfacial layer before deposition of Al cathode;[7-11] and (ii) use of a thin interfacial cathode with a low work function such as Ca or Ba prior to deposition of the Al layer.[12] The non-metallic interfacial layers include thin metal fluoride layers,[10,11] thin polymeric layers,[7-9] metal oxide layers,[16-18] and *n*-doped layers.[18] In this paper, we discuss the effects of the interfacial layers and low work function metals on the short-circuit current (J_{sc}) as well as on the open-circuit voltage (V_{oc}) and the fill factor (FF).

2. EFFECTS OF INTERFACIAL LAYERS FOR EF FICIENT ELECTRON EXTRACTION

2.1. Thin metal fluoride layer

In order to provide an efficient injection or electron extraction contact, metals with a low work function such as Ca or Ba can be used for OLEDs or OPVs.[6,12,19-22] Since these

metals are highly reactive to oxygen and moisture, and thus tend to degrade quickly without reliable encapsulation,[21,22] a thin metal fluoride layer combined with a pure metal layer such as LiF/Al and CsF/Al has been alternatively used for cathodes or negative electrodes.[6,10-12, 20-22] To date, the effect of a metal fluoride layer (e.g. LiF and CsF) in OLEDs has been extensively studied.[20,23-25] However, only a few papers have reported on the effect of the metal fluoride layer on electron extraction in OPVs.[10-12] Therefore, it is important to elucidate the roles of the metal fluoride layer from the viewpoint of electron extraction in the devices.

The metal fluoride layer provides an efficient and stable electron injection contact, even though metal fluorides are insulators.[20,23-28] Since Al and metal fluorides are easier to handle compared with low work function metals, metal fluoride/Al cathodes are generally used for the fabrication of OLEDs.[20,23-28] The underlying mechanisms and the role of metal fluorides in electron injection are still under investigation. Three major models to explain efficient electron injection have been proposed: a reaction model,[20,27] a dipole-moment model,[28] and a tunneling model.[25] In the reaction model, free metal atoms are released from the metal fluoride to the interface upon evaporation of hot reactive metals, which lowers the work function of the cathode. As for the dipole-moment model, since LiF and BaF_2 have high dielectric constants (9.1 and 7.33 @ 1 MHz, respectively), it has been suggested that the large dipole moment in the thin fluoride layer (e.g. 6.33 D for LiF) decreases the surface potential of the aluminum cathode and thus the effective work function, resulting in favorable electron injection.[28] Finally, in the tunneling model, a thin metal fluoride layer can also enhance electron injection by lowering the effective energy barrier within the tunneling range as the metal fluoride layer reduces the effective electric field in the emitting layer, and thus band banding of the emitting layer is reduced.[25] While the exact mechanism for efficient electron injection in this system, however, is still under debate, persuasive evidence suggesting that the reaction model is prevailing has been reported.[20,27] For example, LiF/Ca/Al and BaF_2/Ca/Al cathodes showed more efficient electron injection than LiF/Al and BaF_2/Ba cathodes due to a reduction of the injection barrier height.[6,27]

Cathode engineering involving the use of a metal fluoride layer is very important in OLEDs from the viewpoint of device efficiency and lifetime. Therefore, it is important to study the roles of metal fluoride in electron extraction and device stability in OPVs. According to a recent paper related to cathode engineering in OLEDs, the BaF_2 thickness did not significantly affect the electron injection and the luminous efficiency at a thickness range beyond the monolayer (~ 3 nm for BaF_2).[6] Figure 3 shows atomic force microscope (AFM) images of thermally evaporated BaF_2 on a semiconducting polymer film with varying thickness, monitored with a
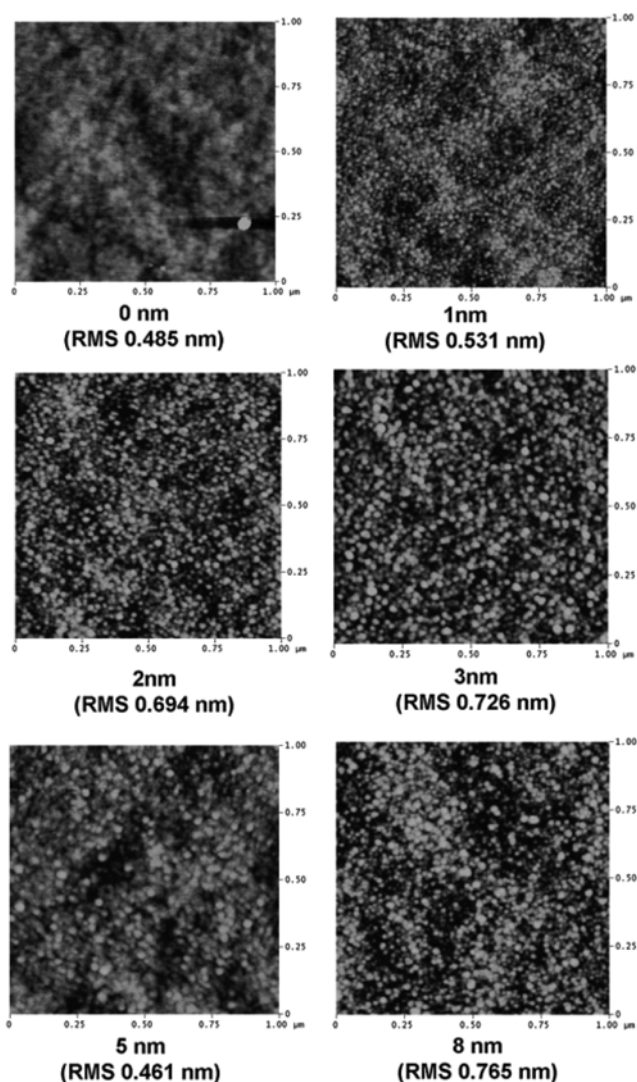
Fig. 3. Atomic force microscope images of thermally evaporated BaF$_2$ on the blue emitting polymer film with varying thickness. Root mean square (RMS) roughness values are indicated. (Reprinted with permission from [6] © 2009 copyright Wiley-VCH)

quartz crystal microbalance sensor, reported by Lee *et al.*[6] The grain size of BaF$_2$ tends to increase as the deposited thickness increases. BaF$_2$ shows island growth on the polymer surface. Accordingly, the root-mean-square (RMS) roughness increased from 0.531 (1 nm thickness) to 0.726 (3 nm thickness). However, for a 5 nm thick film, the RMS roughness decreased to 0.461 nm. This implies that small grains start to grow between the large grains after formation of one monolayer, which results in the void being filled between the large grains. Again, the RMS roughness increased to 0.765 nm for an 8 nm thick film. From these AFM results, it was concluded that BaF$_2$ forms a single monolayer at around 3 nm thickness.

Although the metal fluoride itself is insulating, high oper-

ating voltage above 2 V in OLEDs can cause the electrons to tunnel through the thin fluoride layer up to a certain thickness even above the monolayer. However, in the case of OPVs, the situation could be different. The open circuit-voltage through the devices (usually 0.5 V to 0.8 V) is not as high as the operating voltages in OLEDs (usually > 3 V). When a metal fluoride layer having a thickness above the monolayer thickness is applied, the series resistance in OPVs could be improved. Therefore, it is very important to observe whether the surface is evenly covered by the metal fluoride and to determine the monolayer thickness. The metal fluorides follow the island growth mechanism (Volmer-Weber),[6,27] and thus the film is not uniform. Therefore, the effective work function of the metal fluoride/Al cathode becomes very dependent on the nominal thickness of the metal fluoride.[27]

Recently, Ahlswede *et al.* reported a comparative study of the influence of LiF, NaF, and KF on the performance of OPVs. Interestingly, as the thickness increases up to 1.8 nm, the PCE of OPVs using a NaF or KF interfacial layer dramatically decreases, while that using LiF increased to the optimum level at around 0.6 nm to 1.2 nm and then decreased again. Since they did not perform experiments with thicker films above 1.8 nm, it is difficult to draw a clear conclusion from the results. Chen *et al.* reported the effect of a CsF interlayer on the performance of polymer bulk heterojunction solar cells. They found that the device performance showed quite similar PCEs within a thickness range from 0.4 nm to 3.0 nm, while the device with a LiF interlayer showed a significantly reduced PCE at 2.0 nm.[11] From these results, we can conclude that the power conversion efficiencies of OPVs critically depend on the kinds and the thickness of the metal fluoride interlayers. On the other hand, the luminous efficiency of OLEDs as a function of the thickness showed different characteristics. The luminous efficiency was not changed significantly depending on the thickness of the metal fluoride, but rather the device stability was quite dependant on the thickness.[6] Therefore, since the metal fluoride in OPVs affects the device performance differently as compared to OLEDs, it is necessary to investigate the mechanism of electron extraction from the photoactive layer.

2.2. Thin polymeric layer

To provide an efficient extraction contact in OPVs, an approach incorporating a thin polymeric layer instead of metal fluorides at the interface of the active layer/metal (Al, Ag, or Au) is also promising, as the layer can be processed by a simple solution process.[7-9] To realize flexible organic solar cells at low cost and via a simple non-vacuum process, an air-stable cathode such as Al, Ag, or Au should be employed. In this regard, a solution-processible electron extraction layer on top of the active layer is required for efficient electron extraction in air-stable devices. In OLEDs, many cathode interfacial layers using a solution process

have been developed to improve electron injection. Ionic polymers such as ionomers,[2] single ion conductors,[1,3] ionic salt-containing polymers,[4] and polymer electrolytes[5] have been effectively employed in polymer OLEDs. These polymers are beneficial as they do not smear the underlying active layer due to their good solubility in polar solvents such as alcohol, dimethyl formamide, and water. The primary role of these ionic polymers in OLEDs is to lower the electron injection barriers due to the interfacial dipoles between the emitting layer and the metal cathode. As a result, the interfacial layer has improved the device luminous efficiency greatly.

In OPVs, several approaches using a thin polymeric layer between the active layer and the metal negative electrode have been reported. Inganäs *et al.* reported that when thin poly(ethylene oxide)(PEO) (1 nm to 2 nm) was incorporated between the active layer and the Al electrode, the V_{oc}, FF, and PCE were greatly improved.[7] Figure 4 shows that the V_{oc} values increase significantly in all diodes with PEO, by 150 mV to 200 mV, irrespective of the thickness of the layer. FF values monotonically increased with a decrease of the thickness of PEO. Overall performance was considerably improved in all diodes with application of PEO as a buffer
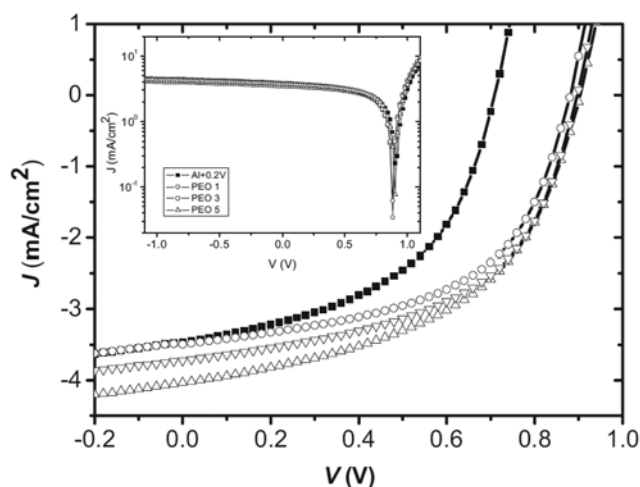

Fig. 4. The J-V characteristics of the diodes with electrodes of PEO/Al and Al, where the line with squares is for the device with the Al electrode, circles are for the device with the PEO1/Al electrode, up-triangles are for the device with the PEO3/Al electrode, and down-triangles are for the device with the PEO5/Al electrode. The inset is a replot of Fig. 4 by shifting the bias for the device with the Al electrode by 200 mV. They measured the thicknesses of the PEO layers on Si wafers by using ellipsometry, with samples prepared under the same deposition conditions as in device fabrication. The thicknesses are 3.8 nm for 1000 rpm, 2.1 nm for 3000 rpm, and 1.4 nm for 5000 rpm. The thicknesses of the PEO layers in devices should not be thicker than those on the Si wafers because the surfaces of the active layers are more hydrophobic than those of the Si wafers. Therefore, the thickness of the PEO layer in devices is estimated to be in the range of 1 nm to 2 nm. (Reprinted with permission from [7] © 2009 copyright Wiley-VCH).

layer beneath Al. An improvement of the PCE by more than 50% was attained in the best diodes. By replotting photocurrent data from the different diodes, and shifting the Al cathode data by the extra photovoltage, a good overlap of the current–voltage characteristics for all variants is found (inset of Fig. 4). It appears that the collection of charge carriers is largely the same, with the difference being attributed to the presence of an internal field. The shift of 0.2 V found in the Al cathode device could be related to internal dipoles at the blend/Al interface. The enhanced FF with an interfacial layer of PEO may be attributed to the distribution of an internal electric field, which facilitates charge transport from active layers to electrodes.

Recently, several groups have attempted to incorporate alcohol/water-soluble polyelectrolytes to improve the PCE of OPVs.[8,9,30] It has been reported that such an interlayer between the active layer and a high work function cathode such as Al, Ag, or Au can significantly improve the charge injection and the luminous efficiency of polymer light-emitting diodes.[5,31,32] Figure 5 shows the chemical structures of alcohol/water-soluble conjugated polyelectrolytes that can be employed for OPVs as well as OLEDs. Cao *et al.* reported that the V_{oc} of polymer solar cells can be enhanced by 0.3 V via insertion of a thin polyelectrolyte layer (**P2**). They attributed this enhancement to the superposition of a built-in-field with the interfacial dipole of the interlayer.[30] Kim *et al.* reported that poly[(9,9-bis((6′-(*N*,*N*,*N*-trimethylammonium)hexyl)-2,7-fluorene)-*alt*-(9,9-bis(2-(2-methoxyethoxy)ethyl)-fluorene))dibromide (**P4**) can be effectively used as an interlayer in OLEDs and OPVs.[5,8] The improvement in PCE in OPVs is attributed to the enhanced V_{oc} and FF resulting from a reduction of the metal work-function through introduction of the conjugated polyelectrolyte.[8] Xie *et al.* reported that incorporation of ethanol-soluble conjugated polyfluorene (**P5**) as an interlayer between the active layer and the Al cathode increases the shunt resistance and improves the photo-generated charge collection.[9] One interesting aspect for OPV devices using a polyelectrolyte interlayer is that the PCE was improved primarily by enhanced V_{oc}. The layer had little effect on the J_{sc}. Therefore, the improvement in PCE by using the polymeric interlayers likely originates mainly from enhancement of the effective work function, which increases the built-in-potential in the devices.

2.3. Metal oxide layer

In addition to thin polymeric layers soluble in polar solvents , solution processible metal oxide precursors and nanoparticles can be effectively employed as an electron extraction layer and optical spacer in OPVs.[16,17] They include *n*-type semiconducting oxides such as TiO_x[16] and ZnO.[17] It is well known that titania (TiO_2) has a substantial oxygen/water protection and scavenging effect, originating from a combina-
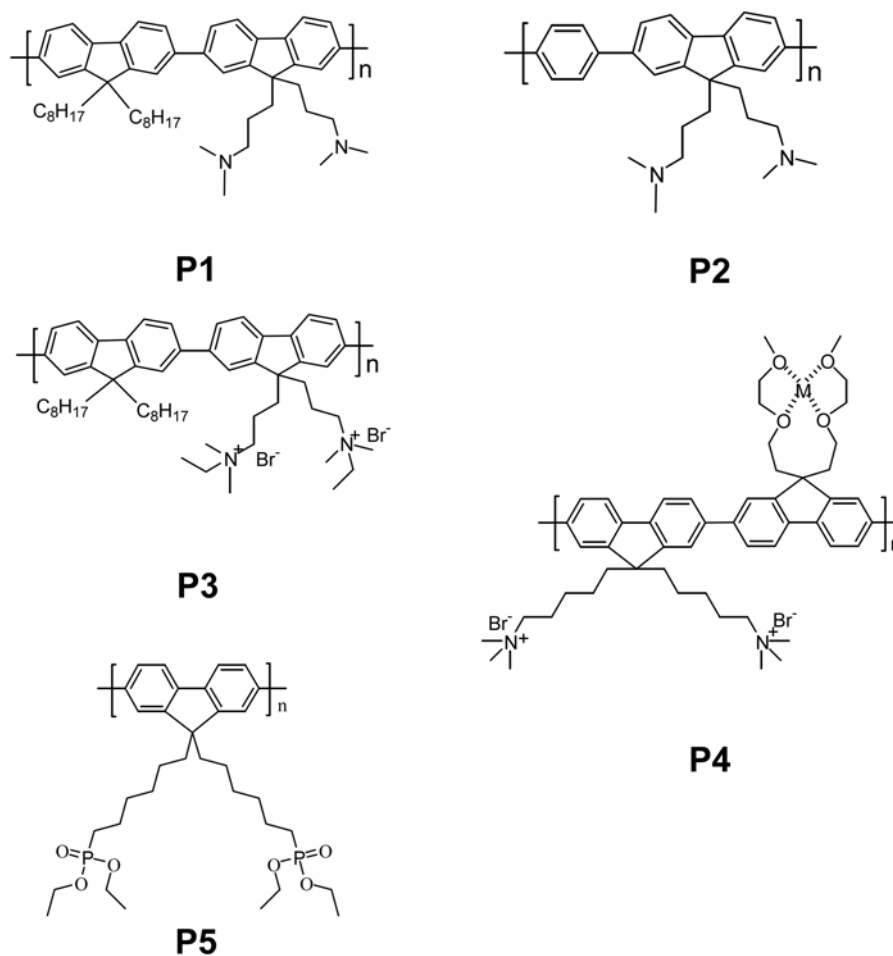
Fig. 5. The chemical structures of alcohol/water-soluble conjugated polyelectrolytes, which have been used as an interlayer between the active layer and the high work function cathode in OLEDs and OPVs. P1: Poly[(9,9-bis(3'-(*N,N*-dimethylamino)propyl)-2,7-fluorene)-*alt*-2,7-(9,9-dioctylfluorene)] (PF-NR2),[31-33] P2: Poly[(9,9-bis(3'-(*N,N*-dimethylamino)propyl)-2,7-fluorene)-*alt*-1,4-phenylene],(PFPNBr),[30,31] P3: Poly[(9,9-bis(3'-((*N,N*-dimethyl)-N-ethylammonium)-propyl)-2,7-fluorene)-alt-2,7-(9,9-dioctylfluorene)]Dibromide (PF-NR3+Br-),[31-33] P4: poly[(9,9-bis ((6'-(*N,N,N*-trimethylammonium)hexyl)-2,7-fluorene)-*alt*-(9,9-bis(2-(2-methoxyethoxy)ethyl)-fluorene))dibromide, bound with mobile alkali or alkaline earth metal ions without their counter ions (M-WPF-oxy-F) (M^+: Na^+, Ca^{2+}),[5,8] P5: Poly(9,9-bis(6'-diethoxylphosphorylhexyl)fluorene)(PF-EP).

tion of photocatalysis and inherent oxygen deficiency.[34–37] Therefore, from the viewpoint of device lifetime, the incorporation of TiO_2 into polymer devices can be a useful approach toward reducing the sensitivity of such devices to oxygen and water vapor. However, since crystalline TiO_2 layers typically can only be prepared at temperatures above 450°C, the process cannot be applicable to general low temperature appraoches in organic electronics. A solution-based sol-gel process of a titanium sub-oxide (TiO_x) layer can be performed on top of polymer-based active layers to provide an electron transport/injection layer for PLEDs[38] and an electron extraction layer and optical spacer for OPVs.[39] Lee *et al.* have demonstrated that both the device performance and the device lifetime are significantly enhanced.[16] The device architecture is shown in Fig. 6.

Because of optical interference between the incident (from the ITO side) and back-reflected light, the intensity of the light is zero at a metallic (Al) electrode without an optical spacer. Figure 7(a) shows a schematic representation of the spatial distribution of the squared optical electric-field strength.[39] Thus, in the device without the optical spacer, a relatively large fraction of the active layer is in a dead-zone in which the photogeneration of carriers is significantly reduced. Moreover, this effect causes more electron–hole pairs to be produced near the ITO/PEDOT:PSS electrode, which is known to reduce the photovoltaic conversion efficiency.[40,41] In order to overcome these problems, the thickness of the active layer could be increased so as to absorb more light. Because of the low mobility of the charge carriers in the polymer:C60 composites, however, the increased internal resistance of thicker films will inevitably lead to a reduced FF. An alternative approach is to change the device
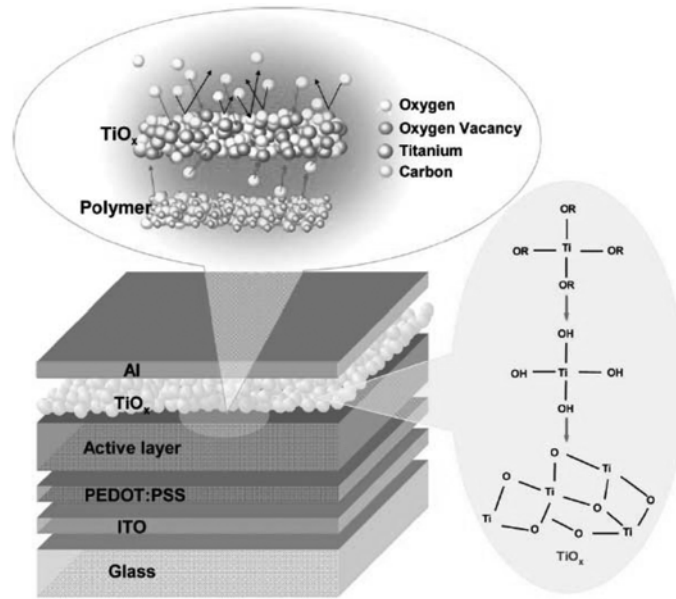
Fig. 6. A schematic device architecture of organic solar cells using the TiO_x layer. The TiO_x functional layer is inserted as an electron extraction and optical space layer between the active layer and the Al electrode with a structure of ITO/PEDOT:PSS/Active Layer/TiO_x/Al. The TiO_x layer acts as a shielding and scavenging layer which prevents the intrusion of oxygen and humidity into the electronically active polymers. A brief flow chart of the steps involved in the preparation of the TiO_x layer is also shown. (Reprinted with permission from [16] © 2007 copyright Wiley-VCH).
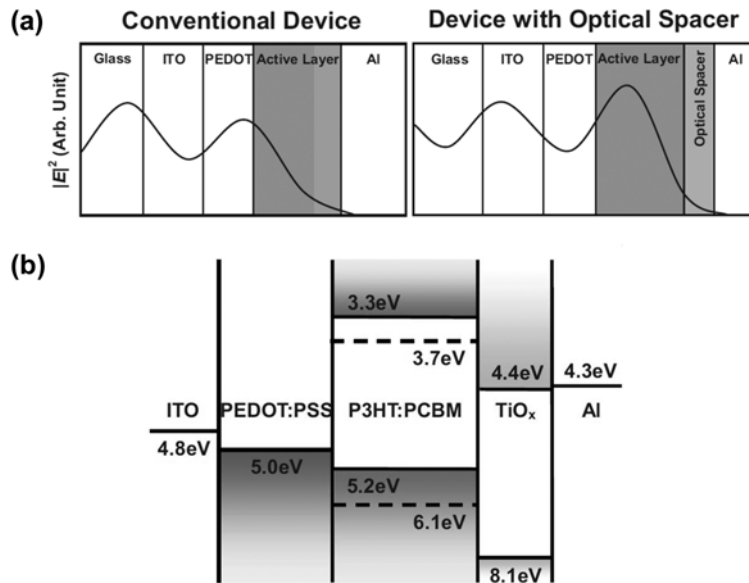

Fig. 7. (a) Schematic representation of the spatial distribution of the squared optical electric field strength $|E|^2$ inside the devices with a structure of ITO/PEDOT/active layer/Al (left) and ITO/PEDOT:PSS/active layer/optical spacer/Al (right). (b) The energy levels of the single components of photovoltaic cell in the structure of ITO/PEDOT:PSS/P3HT:PCBM/TiOx/Al are also shown. (Reprinted with permission from[39] © 2006 copyright Wiley-VCH).

architecture with the goal of spatially redistributing the light intensity inside the device by introducing an optical spacer between the active layer and the Al electrode, as illustrated in Fig. 7(a).[39] The optical spacer must be transparent to light with wavelength within the solar spectrum, should be a good acceptor, and should be an electron-transport material with a conduction band edge lower in energy than that of the lowest unoccupied molecular orbital (LUMO) of C_{60} or PCBM. As shown in Fig. 7(b), TiO_x has no optical absorption in the visible wavelength range due to its large band gap (3.7 eV) and the conduction band edge level (-4.4 eV) is lower than the LUMO level of PCBM (-3.7 eV), which facilitates efficient

electron transfer and extraction from the polymer:fullerene blend. In addition, the low-lying valence band of TiO_x can also effectively prevent hole carriers in the polymer from reaching the cathode. TiO_x is *n*-type doped to relatively high levels, as inferred from an analysis of X-ray photoelectron spectroscopy (XPS) data (Ti:O = 42.1:56.4 in percent or 1:1.34 rather than 1:2 for TiO_2).[16]

It is well known that deficient oxygen sites act as electron donors in this class of materials, thus providing a relatively high density of electron carriers for *n*-type transport.[42] In spite of its amorphous nature, as confirmed by X-ray diffraction, the electron mobility (μ_e) measured by time-of-flight measurements was $\sim 1.7 \times 10^{-4}$ cm^{2}V^{-1}s^{-1}, which is somewhat higher than that of typical sol-gel processed amorphous oxide films.[39] Nevertheless, the electrical properties of TiO_x films are strongly dependent on the processing conditions. The μ_e value is two to three orders of magnitude lower than that of high-performance organic semiconductors used in the active layer (e.g. pentacene, P3HT). This might be a potential limiting factor for high-efficiency devices.[43]

At this point, it is important to note the following. The device using TiO_x layer showed improvement in all the parameters of V_{oc}, J_{sc}, and FF. On the other hand, although the devices using a thin polymeric layer showed great improvement in V_{oc} and slight improvement in FF. they did not show significant improvement in J_{sc}. Therefore, the improvement in all the parameters using TiO_x indicates that the *n*-type TiO_x layer contributes to increased photocurrent by acting as an optical spacer as well as a good electron extractor or transporter.

Taking an approach similar to methods using TiO_x, Jen *et al.* have incorporated a solution-processed thin film of zinc oxide nanoparticles (ZnO NPs) as an alternative electron transporting interlayer.[17] ZnO is a large-bandgap *n*-type semiconductor that has a conduction band and valence band edge level equal to -4.4 eV and -7.6 eV relative to vacuum, respectively.[44] Similar to TiO_2, the conduction band edge of ZnO is lower in energy than that of the LUMO of PCBM.[45] They also systematically tuned the contact properties between the ZnO and metal by interfacial modification with a series of carboxylic-acid-based dipolar SAMs.[17] With an appropriate choice of SAM molecules on ZnO, the OPVs showed dramatically improved efficiencies (4.21%) even with high-work-function electrodes such as Ag and Au.

3. EFFECT OF LOW WORK FUNCTION METALS FOR EFFICIENT ELECTRON EXTRACTION

The effect of metal cathodes on the performance of OLEDs has been extensively studied.[6,46,47] It is well known that a lower work function cathode in OLEDs provides more electrons into the active organic layer, and thus the luminous efficiency tends to be more enhanced.[46] Brabec *et al.* reported on the

effects of negative electrodes on OPVs using poly(2-methoxy-5-(3′,7′-dimethyloctyloxy)-1,4-phenylenevinylene)(MDMO-PPV):PCBM blend as a photoactive layer.[48] Figure 8(a) shows the photocurrent density versus voltage curves of four typical OPV devices utilizing Ca, Al, Ag, and Au as negative electrodes, whose work functions correspond to 2.87, 4.28, 4.26, and 5.1 eV, respectively.[48] A total variation of less than 200 mV for the V_{oc} was observed for variation of the negative electrode work function of more than 2.2 eV. For the devices with an Au electrode, V_{oc} was found to remain as high as 650 mV, which is slightly lower than the average value, while the Ca devices exhibited a V_{oc} of 814 mV. It should be noted that the direction of flow of the short circuit current was not reversed in the case of the Au electrode. In this device, holes still flow toward the ITO/PEDOT:PSS electrode (positive electrode), while electrons are still collected at the (negative) Au electrode. This can be
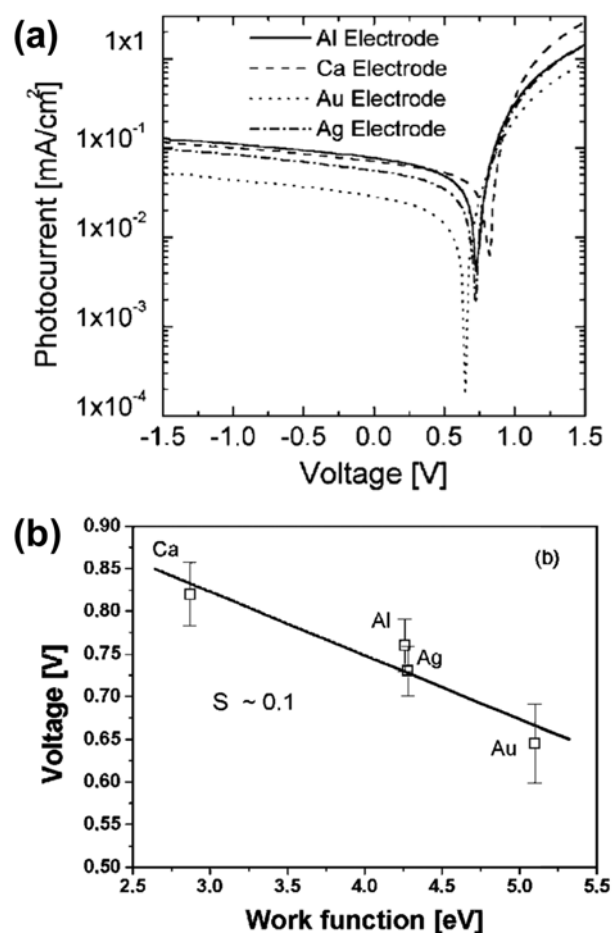

Fig. 8. (a) Photourrent density versus voltage characteristics for MDMO-PPV:PCBM photovoltaic devices with different metal electrodes. Al electrode (solid line), Ca electrode (dashed line), Au electrode (dotted line), Ag electrode (dash-dotted line). (b) Voc versus negative electrode work function. The slopes S of the linear fits to the data are given inside the figures. (Reprinted with permission from[48] © 2001 copyright Wiley-VCH).

understood based on Fermi-level pinning between PCBM and the negative metal electrode.[48] It is observed that the short circuit current for the Au devices is clearly lower than for comparable devices with other electrodes, indicating the importance of the work function of negative electrodes for efficient electron extraction. On the other hand, although the J_{sc} of the Ca device is quite similar to that of the Al device, the current-density at positive bias is significantly higher than that of the Al device. This implies that the electron extraction process in OPVs is somewhat different from the electron injection process in organic diodes.

The influence of the work function of the negative electrode on the V_{oc} of the OPVs is shown in Fig. 8(b). It is important to note that the x-axis now covers more than 2 eV. A linear model was fitted to the experimental data and a slope S ~ 0.1 was calculated as the best fit.[48] Since the slope can be interpreted as the interface parameter that reflects the correlation between x and y axis in a range of $0 \leq S \leq 1$ (for S = 0, the negative electrode is completely pinned to the LUMO levels of the acceptor), the result implies that the V_{oc} has considerably weaker dependence on the work function of the negative electrode compared with the dependence on the LUMO (or reduction potential) of the fullerene derivative.[48] However, when the work function of the negative electrode is below the LUMO level of the acceptor, J_{sc} is critically dependant on the work function, indicating nonlinear dependence. As a result, the PCE becomes more largely dependent on the work function of the negative electrodes.

The device lifetime of OLEDs is not necessarily dependant on the cathode work function. In polymer light-emitting diodes, the ionic radius of cathode metal with alkali and alkaline earth metals is a much more important factor than their work functions in terms of device lifetime.[49] Among alkali and alkaline earth metals, a device with a larger ionic radius metal showed longer device lifetime, and a Ba cathode (ionic radius:1.42 Å) in particular provided the best lifetime in PLEDs; this could be attributed to reduced mobility of the larger metal atoms into the emitting layer film. Since the diffused metal atoms during operation can act as luminescence quenching centers,[50-52] they are one of the critical factors affecting the luminance drop during the operation. In the case of OPVs, the internal electric field corresponding to a built-in-potential inside the devices is much lower than the usual operating voltages of OLEDs for application to flat-panel displays and solid-state lighting devices. Therefore, the diffusion of metal ions into the active layer might not be critical in terms of degradation of OPV devices.

Recently, Reese *et al.* reported the degradation of P3HT: PCBM photovoltaic devices with varying the cathode. They suggested that the active layer may be quite robust, and the interfaces may be responsible for a significant amount of the overall degradation.[52] It should be noted that an air stable Ag cathode showed significant degradation with time even

without illumination, whereas air unstable Ca/Al and Ba/Al cathodes showed much slower degradation with time under the same conditions. The authors concluded that the OPV devices follow interfacial degradation modes rather than inherent active layer degradation. Therefore, at the current stage of research in OPVs, it is very important to investigate in detail the degradation modes at various interfaces in order to prolong device lifetime.

4. SUMMARY AND OUTLOOK

We have discussed the roles of non-metallic interfacial layers, such as thin metal fluorides, thin polymeric layers, and solution processed metal oxide layers, at the interface between the photoactive layer and the negative electrode for an efficient and stable electron extraction contact in bulk heterojunction OPVs based on polymer : fullerene blends. In addition, we have discussed the roles of metallic negative electrodes in OPVs in terms of device efficiency and lifetime. Incorporation of thin metal fluorides as an interlayer is also a common approach in OLEDs. However, the effect of the thickness of the metal fluorides in OPVs appears to be quite different from that in OLEDs; this originates from the insulating nature of metal fluorides and their lower internal electric field compared with the operating voltages in OLEDs.

A thin polymeric interlayer has been effectively used for polymer light-emitting diodes as well. While the same polymeric interfacial layers can be employed in OPVs, they have a more pronounced effect on the V_{oc} compared with the J_{sc}. Therefore, it is necessary to identify appropriate polymeric materials to enhance the J_{sc} as well to further improve the PCE. To this end, a worthwhile direction of research may be to identify an electron-transporting polymer whose LUMO level is lower in energy than that of the acceptor (fullerene).

Application of a solution processible metal-oxide layer is also a promising approach to improve the device performance. In particular, in devices using a TiO_x interlayer, the J_{sc} was greatly improved as well as the V_{oc} and the FF. This likely originates from TiO_x's good electron extraction capability due to its strong *n*-type character as well as its capacity to spatially redistribute the light intensity inside the device by acting as a transparent optical spacer. We also discussed the effects of metallic negative electrodes on the OPV performance. Since the metal work function becomes pinned to the LUMO level, V_{oc} has weak linear dependence on the electrode work function. However, J_{sc} has a nonlinear dependence on the work function of the negative electrode. As a result the PCE exhibits a more pronounced dependency on the work function of the negative electrode than V_{oc} or J_{sc}.

The device stability issues in OPVs appear to be somewhat different from those in OLEDs. OPV devices do not have a large internal electric field and thus do not go through

the degradation mode caused by strong metal and ion diffusion into the active layer, one of the key differences with respect to the degradation modes of OLED devices. However, similar to OLED devices, the degradation of OPV devices seems to be very dependent on the interfaces rather than the inherent degradation of the active layer. Given that many approaches to improve the device stability as well as the efficiency in OLEDs have been reported, it is anticipated that the optimization of OPV device efficiency and lifetime could be accelerated by modifying the interface at the negative electrode.

ACKNOWLEDGMENTS

REFERENCES

1. T.-W. Lee and O. O. Park, *Appl. Phys. Lett.*, **76**, 3161 (2000).
2. T.-W. Lee, O. O. Park, L.-M. Do, T. Zyung, T. Ahn, and H.-K. Shim, *J. Appl. Phys.*, **90**, 2128 (2001).
3. T.-W. Lee and O. O. Park, *Adv. Mater.* **13**, 1274 (2001).
4. T.-W. Lee, H.-C. Lee, and O. O. Park, *Appl. Phys. Lett.*, **81**. 214 (2002).
5. S.-H. Oh, D. Vak, S.-I. Na, T.-W. Lee, and D.-Y. Kim, *Adv. Mater.*, **20**, 1624 (2008).
6. T.-W. Lee, M.-G. Kim, S. H. Park, S. Y. Kim, O. Kwon, T. Noh, T.-L. Choi, J. H. Park, and B. D. Chin, *Adv. Funct. Mater.,* **19**, 1863 (2009).
7. F. Zhang, M. Ceder, and O. Inganäs, *Adv.Mater.,* **19**, 1835 (2007).
8. S.-I. Na, S.-H. Oh, S.-S. Kim, D.-Y. Kim, *Org. Electron,* **10**, 496 (2009).
9. Y. Zhao, Z. Xie, C. Qin, Y. Qu, Y. Geng, L. Wang, *Sol. Energy Mater. Sol. Cells*, **93**, 604 (2009).
10. S.-H. Lee, J.-H. Kim, T.-H. Shim, and J.-G. Park, *Electron. Mater. Lett.* **4**, 19 (2008).
11. X. Jiang, H. Xu, L. Yang, M. Shi, M. Wang, H. Chen, *Sol. Energy Mater. Sol. Cells*, **93**, 650 (2009).
12. M. O. Reese, M. S. White, G. Rumbles, D. S. Ginley, and S. E. Shaheen, *Appl. Phys. Lett.* **92**, 053307 (2008).
13. T.-W. Lee, T. Noh, B.-K. Choi, M.-S. Kim, D. W. Shin, and J. Kido, *Appl. Phys. Lett.* **92**, 043301 (2008).
14. J. Endo, T. Matsumoto, and J. Kido, *Jpn. J. Appl. Phys.* **41**, L800 (2002).
15. http://www.isiknowledge.com
16. Lee, J. Y. Kim, S. H. Park, S. H. Kim, S. Cho, and A. J. Heeger, *Adv. Mater.* **19**, 2445 (2007).
17. H.-L. Yip, S. K. Hau, N. S. Baek, H. Ma, and A. K.-Y. Jen, *Adv. Mater.* **20**, 2376 (2002).
18. M.-H. Park, J.-H. Li, A. Kumar, G. Li, and Y. Yang, *Adv. Funct. Mater.* **19**, *1241* (2009).
19. T.-W. Lee, Y. Chung, O. Kwon, and J.-J. Park, *Adv. Funct. Mater.* **17**, 390 (2007).
20. M. Y. Chan, S. L. Lai, M. K. Fung, C. S. Lee, and S. T. Lee, *J. Appl. Phys.* **95**, 5397 (2004).
21. M. T. Lloyd, D. C. Olson, P. Lu, E. Fang, D. L. Moore, M. S. White, M. O. Reese, D. S. Ginley, and J. W. P. Hsu, *J. Mater. Chem.* **19**, 7638 (2009).
22. M. O. Reese, A. J. Morfa, M. S. White, N. Kopidakids, S. E. Shaheen, G. Rumbles, D. S. Ginley, *Sol. Energy. Sol. Cells* **92**, 746 (2008).
23. H. Heil, J. Steiger, S. Karg, M. Gastel, H. Ortner, H. von Seggern, and M. Stößel, *J. Appl. Phys.* **89**, 420 (2001).
24. M. Y. Chan, S. L. Lai, M. K. Fung, C. S. Lee, S. T. Lee, *Chem. Phys. Lett.* **374**, 215 (2003).
25. X. J. Wang, J. M. Zhao, Y. C. Zhou, X. Z. Wang, S. T. Zhang, Y. Q. Zhan, Z. Xu, H. J. Ding, G. Y. Zhong, H. Z. Shi, Z. H. Xiong, Y. Liu, Z. J. Wang, E. G. Obbard, X. M. Ding, W. Huang, and X. Y. Hou, *J. Appl. Phys.* **95**, 3828 (2004).
26. X. Yang, Y. Mo, W. Yang, G. Yu, and Y. Cao, *Appl. Phys. Lett.* **79**, 563 (2001).
27. T. M. Brown, R. H. Friend, I. S. Millard, D. J. Lacey, T. Butler, J. H. Burroughes, and F. Cacialli, *J. Appl. Phys.* **93**, 6159 (2003).
28. S. E. Shaheen, G. E. Jabbour, M. M. Morrell, Y. Kawabe, B. Kippelen, N. Peyghambarian, M.-F. Nabor, R. Schlaf, E. A. Mash, and N. R. Armstrong, *J. Appl. Phys.* **84**, 2324 (1998).
29. E. Ahlswede, J. Hanisch, and M. Powalla, *Appl. Phys. Lett.* **90**, 163504 (2007).
30. J. Luo, H. Wu, C. He, A. Li, W. Yang, and Y. Cao, *Appl. Phys. Lett.* **95**, 043301 (2009).
31. F. Huang, H. Wu, D. Wang, W. Yang, and Y. Cao, *Chem. Mater.* **16**, 708 (2004).
32. H. B. Wu, F. Huang, Y. Q. Mo, W. Yang, D. L. Wang, J. B. Peng, and Y. Cao, *Adv. Mater.* **16**, 1826 (2004).
33. H. B. Wu, F. Huang, H. L. Shen, and Y. Cao, *Org. Electron.* **6**, 118 (2005).
34. A. Fujishima and K. Honda, *Nature*, **238**, 37 (1972).
35. A. L. Linsebigler, G. Lu, and J. T. Yates, Jr., *Chem. Rev.* **95**, 735 (1995).
36. V. E. Henrich and P. A. Cox, *The Surface Science of Metal Oxides*, Cambridge University Press, Cambridge (1994).
37. C. Noguera, *Physics and Chemistry of Oxide Surfaces*, Cambridge University Press, Cambridge (1996).
38. S. H. Kim, J. Y. Kim, S. H. Park, and K. Lee, *Proc. SPIE-Int. Soc. Opt. Eng.* **5937**, 59 371G1 (2005).
39. J. Y. Kim, S. H. Kim, H.-H. Lee, K. Lee, W. Ma, X. Gong, and A. J. Heeger, *Adv. Mater.* **18**, 572 (2006).

40. H. J. Snaith, N. C. Greenham, and R. H. Friend, *Adv. Mater.* **16**, 1640 (2004).
41. C. Melzer, E. J. Koop, V. D. Mihaletchi, and P. W. M. Blom, *Adv. Funct. Mater.* **14**, 865 (2004).
42. U. Diebold, *Surf. Sci. Rep.* **48**, 53 (2003).
43. G. Li, V. Shrotriya, J. S. Huang, Y. Yao, T. Moriarty, K. Emery, and Y. Yang, *Nat. Mater.* **4**, 864 (2005).
44. M. Gratzel, *Nature* **414**, 338 (2001).
45. M. C. Scharber, D. Muhlbacher, M. Koppe, P. Denk, C. Waldauf, A. J. Heeger, C. J. Brabec, *Adv. Mater.* **18**, 789 (2006).
46. I. D. Parker, *J. Appl. Phys.* **75**, 1656 (2004).
47. Y. Cao, G. Yu, I. D. Parker, A. J. Heeger, *J. Appl. Phys.* **88**, 3618 (2000).
48. C. J. Brabec, A. Cravino, D. Meissner, N. S. Sariciftci, T. Fromherz, M. T. Rispens, L. Sanchez, and J. C. Hummelen, *Adv. Funct. Mater.* **11**, 374 (2001)
49. J. Birgerson, M. Fahlman, P. Bröms, W.R. Salaneck, W. R. *Synth. Met.* **80,** 125 (1996).
50. V.-E. Choong, Y. Park, Y. Gao, T. Wehrmeister, K. Müllen, B. R. Hsieh, C. W. Tang, *J. Vac. Sci. Technol. A* **15,** 1745 (1997).
51. Y. Park, V.-E. Choong, B. R. Hsieh, C. W. Tang, Y. Gao, *Phys. Rev. Lett.* **78,** 3955 (1997).
52. M. O. Reese, A. J. Morfa, M. S. White, N. Kopidakis, S. E. Shaheen, G. Rumbles, and D. S. Ginley, *Sol. Energy Mater. Sol. Cells*, **92**, 746 (2008).